JVSTB
JOURNAL OF VACUUM SCIENCE AND TECHNOLOGY B

Comparison of positive tone versus negative tone resist pattern collapse behavior

Wei-Ming Yeh, David E. Noga, Richard A. Lawson, Laren M. Tolbert, and Clifford L. Henderson

Citation: J. Vac. Sci. Technol. B **28**, C6S6 (2010); doi: 10.1116/1.3518136
View online: http://dx.doi.org/10.1116/1.3518136
View Table of Contents: http://avspublications.org/resource/1/JVTBD9/v28/i6
Published by the AVS: Science & Technology of Materials, Interfaces, and Processing

Comparison of positive tone versus negative tone resist pattern collapse behavior*

Wei-Ming Yeh, David E. Noga, and Richard A. Lawson
School of Chemical and Biomolecular Engineering, Georgia Institute of Technology, Atlanta, Georgia 30332-0100

Laren M. Tolbert
School of Chemistry and Biochemistry, Georgia Institute of Technology, Atlanta, Georgia 30332

Clifford L. Henderson[a)]
School of Chemical and Biomolecular Engineering, Georgia Institute of Technology, Atlanta, Georgia 30332-0100

(Received 12 July 2010; accepted 29 October 2010; published 30 November 2010)

In this work, e-beam lithography patterns have been specifically designed and fabricated which provide the opportunity to probe the collapse behavior of both positive and negative tone systems. The pattern layout includes adjacent parallel line structures that both vary in the line size and also in the distance by which they are separated by the space between them. This type of structure allows for the control and modulation of the capillary forces, and ultimately the stresses, experienced by the photoresist line pairs during the final rinse and drying steps of the development process. Using such structures, it is possible to determine the critical stress, i.e., the maximum stress experienced by the photoresist lines before collapse, as a function of a variety of parameters including: material type, substrate preparation conditions, resist film thickness, and resist feature width. In this article, such a modular approach has been used to compare the pattern collapse behavior of a prototypical positive tone resist formulated using a protected hydroxystyrene-based copolymer and a prototypical negative tone epoxide-based molecular photoresist (4-EP). It was found that the critical stress at the point of pattern collapse decreased both as the thickness and the feature width of the resist lines decreased, though this trend was observed to a much lesser extent in the negative tone 4-EP material. It is observed that the negative tone resist, whose imaging mechanism involves cross-linking, shows far superior pattern collapse performance as compared to the positive tone deprotection based resist and is in general able to achieve significantly higher aspect ratio patterning at equivalent feature linewidths. [DOI: 10.1116/1.3518136]

I. INTRODUCTION

As the semiconductor industry continues to shrink in size and increase the density of circuit elements in modern integrated circuits, there is tremendous pressure on improving the capabilities of current lithographic processes and materials. Recently, as feature sizes have plunged below 50 nm, problems associated with the collapse of resist patterns have become a much more prominent issue, and in some cases, could serve as the ultimate limiting constraint in terms of the practical resolution for a resist material instead of its inherent ability to respond to radiation and form a relief structure upon development. Pattern collapse, which is a term commonly used to encompass both adhesion failure and line bending and breakage, during wet resist processing is brought about primarily by asymmetric capillary forces experienced by resist features during final drying after development and rinsing. Such asymmetric capillary forces are caused by factors such as asymmetry in the resist pattern spacing itself or uneven drying rates on the wafer. Quantifying and understanding the differences in the collapse behavior of various resist material types, including both positive and negative tone systems and systems based on different polymer or molecular families, can allow for the more efficient development or selection of materials and methods to prevent or mitigate such pattern collapse problems.

The resist materials used in the lithographic process used to fabricate microscopic and nanoscopic systems can be broadly classified into one of two basic types: negative and positive tone resists. Positive tone resists are by far the most common resist type used in high volume integrated circuit manufacturing and are characterized by excellent resolution capabilities (i.e., especially in modern chemically amplified resists) and facile processing, including the use of aqueous developers. Negative tone resists have, over the years, gained a somewhat less favorable reputation due often to the perception that they experience resolution limitations imposed by swelling during development, require organic solvents instead of aqueous solutions for development, and in some cases, suffer from relatively poorer etch resistance.[1] However, negative polymeric resists are used in high volume integrated circuit manufacturing for certain device levels and in applications where the crosslinked nature of many negative systems present an advantage (e.g., in the fabrication of

*No proof corrections received from author prior to publication.

a)Author to whom correspondence should be addressed: electronic mail: cliff.henderson@chbe.gatech.edu

permanent elements in microelectromechanical systems (MEMSs) and microfluidic systems). For example, SU-8 is a very commonly used negative tone resist in MEMS fabrication and is often implemented to form permanent device parts, because it is very stable and difficult to strip.[2] Negative tone polymeric photoresists that utilize the cationic polymerization and crosslinking of epoxide functionalized materials, such as SU-8, have thus, in particular, continued to be used and studied over the years in both electron-beam and deep-UV applications.[3–5] Although improvements in their resolution capabilities have been made over the years, such polymeric cross-linking-based negative resists were until recently seen as having limited potential for future sub-40 nm patterning due to swelling based resolution limitations and other problems. Fortunately, several different types of epoxide functionalized molecular resists have been recently reported with improved lithographic properties.[6–8] In particular, some negative tone epoxide functionalized molecular resists have been shown to have superior lithographic performance to their equivalent polymeric resists,[9] and many such negative tone molecular resists have in fact shown excellent lithographic performance with resolution capabilities down to dense sub-25 nm patterns at sensitivities and line edge roughness equivalent, or better, to other positive tone chemically amplified resists.[10–12] Given this recent possibility of nearly equivalent lithographic performance in terms of resolution, sensitivity, and edge roughness of positive and negative tone resists, the goal of this work was to benchmark their differences with respect to pattern collapse behavior.

Since negative tone resists that function by cross-linking produce essentially a single polymer network of material in the resist feature, it is expected that the mechanical properties of positive and negative tone polymeric resists can be significantly different. In order to further explore the impact, such a difference in the molecular architecture of the resist would have on pattern collapse phenomena, a model positive and negative tone resist system were chosen and compared in this work in terms of their collapse behavior. In a previous work,[13] 1,1,2,2-tetra(4-hydroxyphenyl)ethane tetraglycidyl ether (4-EP) material was found to have excellent resolution, high sensitivity, and extremely low line edge roughness, with nearly equivalent lithographic performance to a variety of the best positive tone chemically amplified resists under both e-beam and extreme ultraviolet (EUV) lithography. Therefore, in this work, the negative tone 4-EP material was chosen as a prototypical future negative tone model resist material. In choosing a positive tone resist material, a resist based on a hydroxystyrene-styrene-acrylate terpolymer was chosen, since it somewhat generically represents a large family of materials being explored for EUV lithography and similar materials had been studied and reported extensively in the literature.

II. EXPERIMENT

A. Materials and equipment

The resin structures of the two resists used in this study are shown in Fig. 1. 4-Ep, propylene glycol monomethyl ether acetate (PGMEA), isopropyl alcohol (IPA), trioctyl amine (TOA), methyl isobutyl ketone (MIBK), and triphenylsulfonium nonaflate (TPS-Nf) were purchased from Sigma–Aldrich. Triphenylsulfonium hexafluoroantimonate (TPS-SbF_6) was purchased from Midori Kagaku Co., Ltd. The particular structure (referred in here as ESCAP-1) of the environmentally stable chemically amplified photoresist resin used in this work is shown in Fig. 1. The ESCAP-1 material was supplied jointly by Japan Synthetic Rubber (JSR) and Intel Corporation. The positive tone resist used in this work was formulated using the ESCAP-1 resin, TPS-Nf photoacid generator (PAG), and TOA as a base quencher. All these components were dissolved in PGMEA at a loading of 7.4 wt% total solids with 5 wt% TPS-Nf relative to ESCAP-1 mass and 10 mol% TOA relative to the TPS-Nf PAG molar content. The 4-EP resists solutions were made by dissolving the 4-Ep molecular resist resin compound along with 5 mol% (with respect to the 4-Ep compound) TPS-SbF_6 PAG into PGMEA. No base quencher was added in the 4-EP resist solutions.

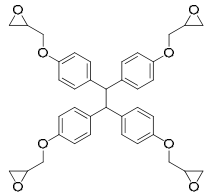

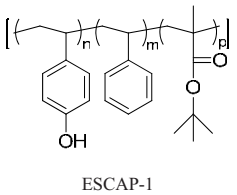

FIG. 1. Chemical structures of the 4-EP and ESCAP-1 photoresist resins used in this work.

The resist processing consisted of first spin coating the resist films at various spin speeds for 60 s to obtain films of varying thickness. The ESCAP-1 films were then subjected to a post-apply bake at 110 °C for 2 min, exposed and patterned via e-beam, subjected to a post-exposure bake at 110 °C for 1 min, developed in 0.26N tetramethylammonium hydroxide for 30 s, rinsed with de-ionized (DI) water for 1 min, and finally dried with flowing nitrogen. The 4-EP films were subjected to a post-apply bake at 90 °C for 1 min, exposed and patterned via e-beam, subjected to a post-exposure bake at 90 °C for 1 min, developed in MIBK for 30 s, rinsed with isopropyl alcohol as a final rinse, and dried with flowing nitrogen.

E-beam lithography was performed using a JEOL JBX-9300FS e-beam lithography system with an accelerating voltage of 100 keV, a beam diameter of 8 nm, a 2 nA current, and a 10 nm shot pitch. Scanning electron microscope (SEM) images were taken using a Zeiss Ultra 60 scanning electron microscope. The resist pattern collapse structures were patterned into resist films coated on hexamethyldisilazane (HMDS) vapor-primed 50 nm thick Si_3N_4 windows supported in a silicon wafer carrier substrate which have been described elsewhere[14] and on bare Si_3N_4 window sub-

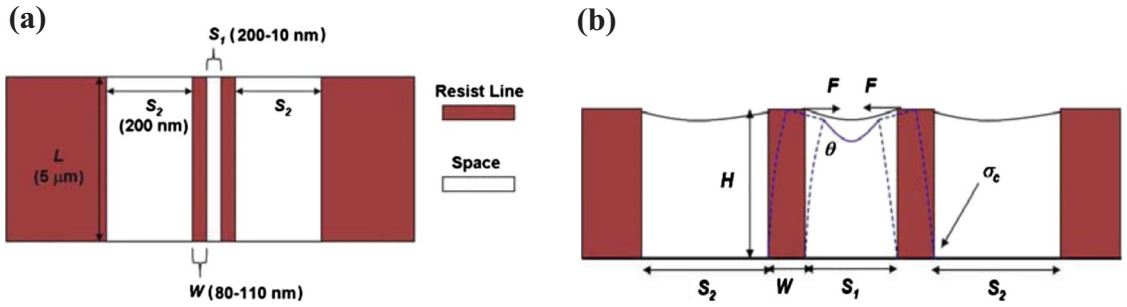

FIG. 2. (Color online) (a) Top view and (b) side view of pattern design used for studying resist collapse behavior and for determining the critical stress at the point of pattern collapse (i.e., the point at which capillary forces become great enough to cause irreversible pattern deformation).

strates that were not subjected to HMDS priming so as to compare the effect of the nature of the substrate surface on the observed collapse behavior.

B. Pattern collapse test structure and collapse analysis

As mentioned previously, an e-beam lithography pattern with a series of varying line and space widths was specifically designed in order to quantitatively study the influence of various material and processing parameters on the resist pattern collapse [Fig. 2(a)]. A pattern collapse is typically caused by unbalanced capillary forces that are experienced by the resist features during the final drying process after resist development and rinse [see Fig. 2(b)]. In this work, these capillary forces are used on purpose to probe the pattern collapse phenomena by intentionally modulating the magnitude of these forces by varying the size of the space widths between and outside a pair of resist lines. In the results shown here, the outside space widths (i.e., S_2) used for all patterns was 200 nm. The inside space widths between each pair of resist lines was varied between 10 and 200 nm in increments of 10 nm.

The initial pressure difference acting on the resist lines can be described using Eq. (1), where γ is the surface tension of the final rinse liquid and θ is the contact angle of the rinse liquid on the photoresist, and S_1 and S_2 are the respective inside and outside space widths between the lines of the pattern. For the surface tensions of the rinse liquids, in the ESCAP-1 case, it is de-ionized water with γ=0.073 N/m and, in the 4-EP case, it is IPA with γ=0.023 N/m. With respect to rinse liquid contact angles on the developed resist feature surface, in the ESCAP-1 case, it was found that de-ionized water exhibited a $\theta = \sim 77°$ when placed on an ESCAP-1 film that had been blanket exposed at a low dose, briefly developed, and rinsed with DI water. In the case of a 4-Ep film that had been coated, blanket exposed, baked, and subjected to developer and rinse, the IPA rinse liquid formed a contact angle on the surface of $\theta = \sim 6°$.

$$\Delta P = 2\gamma \cos\theta \left(\frac{1}{S_1} - \frac{1}{S_2}\right). \tag{1}$$

Using this pressure difference, it is then possible to use solid mechanics to calculate the maximum stress experienced in the resist, which occurs near the bottom corner of the structure where the resist meets the substrate for a resist line with a rectangular cross section, for a given aspect ratio feature and a given set of S_1 and S_2 space widths as shown in Eq. (2). Here, W is the width of the resist feature and H is the thickness of the photoresist film or feature after development.

$$\sigma = 6\gamma \cos\theta \left(\frac{H}{W}\right)^2 \left(\frac{1}{S_1} - \frac{1}{S_2}\right). \tag{2}$$

By looking carefully at the arrays of test patterns for a given resist film sample (i.e., at some particular film thickness of resist) and for a given line width feature, it was possible to determine the smallest S_1 space that could be patterned before the line pair surrounding that S_1 space exhibited pattern collapse of some form. This S_1 value, termed here the critical S_1 width (S_{1C}), can then be used with Eq. (2) to calculate the lower bound on the largest stress that could be supported by the resist features before they experienced collapse. This lower bound on stress before pattern collapse is referred in here as the critical stress at the point of pattern collapse (σ_C) and is calculated as shown in Eq. (3).

$$\sigma_c = 6\gamma \cos\theta \left(\frac{H}{W}\right)^2 \left(\frac{1}{S_{1c}} - \frac{1}{S_2}\right). \tag{3}$$

In this work, the line and space widths of the patterns produced via e-beam lithography after development, rinse, and drying were measured precisely from high resolution SEM images of the structures using custom written MATLAB software designed for high resolution SEM feature analysis.

III. RESULTS AND DISCUSSION

A. Effect of substrate preparation on collapse behavior

With the particular test pattern design used in this work, as the S_1 space width is reduced sequentially from left to right in the pattern array (see SEM image in Fig. 3 for example) for sets of line pairs of constant line width W, the capillary force exerted on the resist structures increases. Ultimately, a pattern collapse occurs at a point in each array when a sufficiently small S_1 value is reached such that the stress applied to the resist exceeds the critical stress required

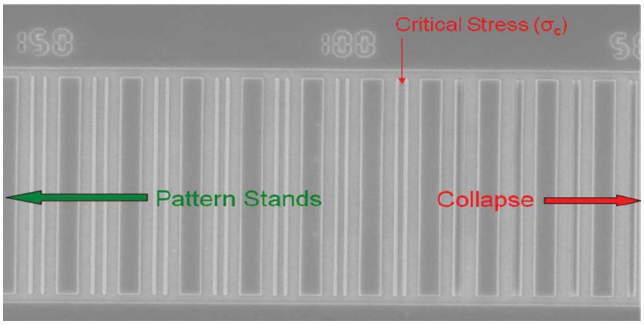

FIG. 3. (Color online) SEM picture of a typical example of the patterned line pair arrays used to study collapse and the corresponding typical pattern failure observed and the method used to identify the critical S_{1c} space width and the corresponding critical stress.

for pattern collapse (see Fig. 3). In this work, it was desired to compare the collapse behavior of the resist materials based on a deformation mode failure as opposed to an adhesion based failure. As a result, studies were performed to identify the influence of substrate preparation condition on the type of collapse observed in these resists.

The Si_3N_4 window substrates with and without HMDS vapor priming were used to compare the effect of substrate condition on the pattern performance. For the ESCAP-1 photoresist, vapor-priming with HMDS prior to spin coating the photoresist resulted in improved resist to substrate adhesion, and the mode of pattern collapse was observed to appear to change to pattern bending and deformation (see Fig. 4) from what appear to be adhesion based failures observed on unprimed substrates. This conclusion is reached because in cases where a pattern collapse is observed in ESCAP-1 on the unprimed substrates, one photoresist line in each line pair at the point where pattern deformation was first observed would clearly detach from the substrate surface and translate across the surface, where it ultimately touches and remains adhered to the adjacent resist line as indicated by the asymmetric nature of the final collapsed structure with respect to the center line of the original line pair (see Fig. 4). In the case of ESCAP-1 on the HMDS primed substrates, the primary mode of failure appeared to be some form of bending of the photoresist lines, which in virtually all cases resulted in a symmetrically collapsed structure that was centered on the nominal center line of the original line pair test structure. Also, the S_1 space widths at the point of collapse were smaller in the case of ESCAP-1 on the HMDS primed substrates, which again support the idea that the adhesion failure mode that was active in the unprimed substrate cases has transitioned to a material deformation mode that requires higher stress in the case of the primed sampled. For 4-EP photoresist, since the films spin coated on the bare Si_3N_4 substrate coat very well and the adhesion of such an epoxide-based material to a surface containing silanol groups is expected to be covalent in nature to some degree, no HMDS priming was used. In looking at the collapsed test structures in 4-Ep, no asymmetric collapse behavior such as that seen in the case of ESCAP-1 on the unprimed substrates was found. Thus, it was again concluded that failure in the 4-Ep samples was by some form of pattern bending mode.

B. Comparison of critical stress behavior

As discussed earlier, for all further studies reported here, the ESCAP-1 resist was coated and patterned on HMDS primed silicon nitride surfaces, while the 4-Ep resists were coated and patterned on unprimed silicon nitride surfaces. As has been previously shown, the imaging of the resists on the specially made thin silicon nitride window substrates provide a nearly electron transparent substrate that prevents any significant electron backscatter from the substrate, which in turn results in extremely vertical sidewalls in the patterned resist structures using the 100 keV exposure system employed here. Such precise resist wall profile control is important if

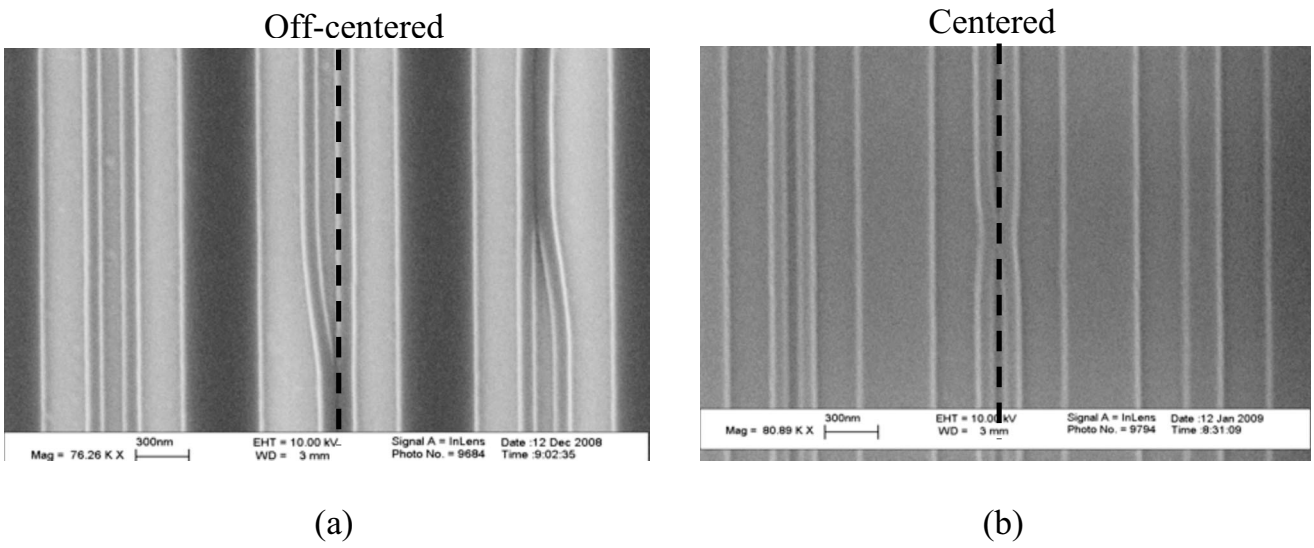

FIG. 4. Effect of HMDS priming of the SiN substrate on the pattern collapse behavior of ESCAP-1 photoresist. (a) Collapse on substrates not treated with HMDS and (b) collapse behavior on substrates treated with HMDS.

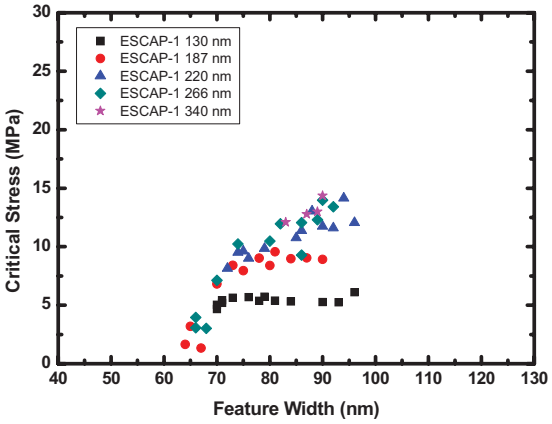

FIG. 5. (Color online) Experimentally determined critical stress at the point of pattern collapse for the positive tone ESCAP-1 photoresist on an HMDS primes surface as a function of resist feature height and width.

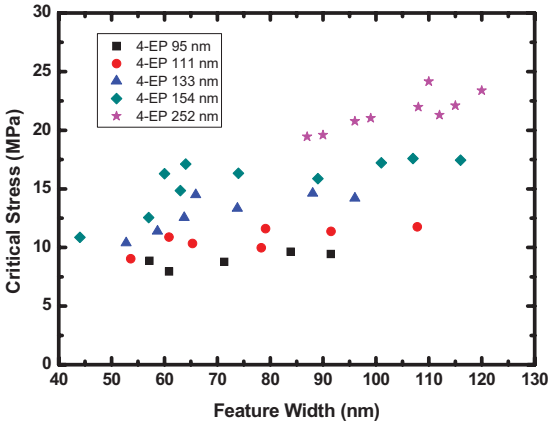

FIG. 6. (Color online) Experimentally determined critical stress at the point of pattern collapse for the negative tone 4-EP photoresist as a function of feature height and width.

one is to be able to utilize the equations presented earlier for calculating the stresses experience in the resist lines.

The critical stress as a function of feature height and width for ESCAP-1 is shown in Fig. 5. The critical stress when collapse occurs in ESCAP-1 is clearly observed to reduce as the resist feature width is reduced. This behavior is qualitatively consistent with studies of the modulus behavior of polymer ultrathin films[15] which suggest that the apparent modulus of polymer thin films and nanostructures should reduce dramatically below some critical thickness. In thin film studies using thin film buckling to determine the modulus of polystyrene and PMMA films, the critical film thickness below which substantial changes in the effective polymer film modulus were observed were on the order of 40 nm. Interestingly, the feature width at which one observes a dramatic decrease in the critical stress at the point of collapse in ESCAP-1 is on the order of 70–80 nm in line structures with two free surface interfaces in the lateral direction of this measured feature width, which is roughly twice the 40 nm length scale observed in polymer films with only one free surface interface.

The critical stress as a function of feature height and width for the 4-EP resist is shown in Fig. 6. Unlike the ESCAP-1 resist, it is observed that the critical stress in the crosslinked 4-Ep resist shows significantly less dependence on resist feature width. This would again be somewhat expected and consistent with the earlier discussion of the thin polymer film modulus behavior. The modulus behavior in thin polymer films thus far has been explored in detail only for noncrosslinked materials and the observed decrease in modulus with reducing film thickness is explained in terms of a lower modulus surface layer that is present in the polymer due to higher chain mobilities near the free interface. In the case of cross-linked materials such as 4-Ep, no such strong variation in local mobility or modulus would be expected for polymers near an interface since the entire film is essentially one large network polymer after it patterned. Somewhat surprisingly, the critical stress at the point of collapse was observed to exhibit a minor dependence on film thickness. The origins of this dependence of critical stress on film thickness in this crosslinked material and other similar materials that are crosslinked after coating are still under investigation.

Figure 7 shows a comparison of the critical stress behavior of ESCAP-1 and 4-EP patterns for films approximately 130 and 260 nm thick. Two important observations are made in considering this data. First, the critical stress required to result in pattern collapse for the crosslinked 4-Ep is substantially larger at an equivalent film thicknesses than in the case of the ESCAP-1 material, with the 4-Ep critical stresses being larger by a factor of roughly 2–3. Second, if one looks at the trend of critical stress with feature width, the ESCAP-1 material exhibits a significant drop off in critical stress as feature widths are reduced below feature widths on the order of 70–80 nm. In contrast, the 4-Ep material exhibits a relatively weak if any dependence of critical stress on feature width. This is in qualitative agreement with the patterning experiments since although line features smaller than 60 nm could be imaged and produced in the ESCAP-1 material, under no processing conditions could these smaller line

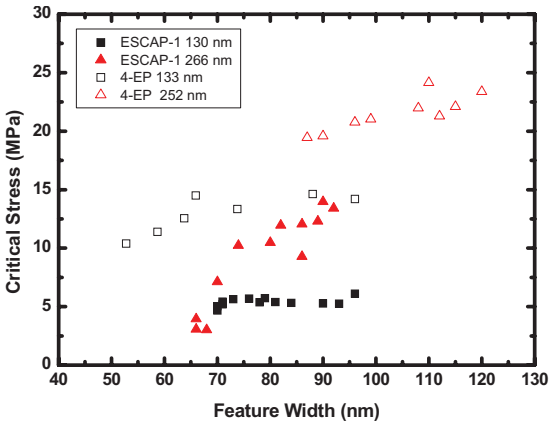

FIG. 7. (Color online) Comparison of the critical stresses of ESCAP-1 and 4-EP photoresist at nominally similar initial film thicknesses (i.e., ~130 and ~260 thick films).

structures be found to survive rinsing and drying without collapsing for any structures in the pattern including virtually isolated lines. In contrast, the structures could be easily patterned into the 4-Ep material down to 40 nm in size, below which feature dimension, it is difficult to cleanly image smaller features under the processing conditions used without the incorporation of other additives to control the cationic polymerization chain length. Comparing the critical stresses at the point of collapse for the prototypical negative and positive photoresists explored in this work, it is clear that negative tone resists based on cross-linking mechanisms are likely to exhibit a far superior pattern collapse behavior as compared to conventional positive tone resist systems. Although it may be tempting to think of the nonadhesion based failure in terms of an elastic deformation, and thus, attribute this difference to the fact that the crosslinked polymeric resist system would exhibit a higher Young's modulus than the noncrosslinked polymeric resist, this view is likely incorrect. Prior studies have shown that the Young's modulus in noncrosslinked vs crosslinked polymer systems of similar types are in fact generally similar in nature, especially at small strains. Instead, it is more likely the case that the failure modes observed in this work are in fact elastoplastic in nature, and thus, it has differences in the yield stress of the two materials, which may be the important factor that results in the large difference in collapse behavior. It would be expected that a crosslinked material would have a higher yield stress than a noncrosslinked system, as the breaking of covalent bonds is required for any significant yielding in the case of the crosslinked material. In fact, the heavily crosslinked 4Ep resist may not even have a significant yield at all, and thus, may instead fail by a brittle mode failure as has been observed in other heavily crosslinked glassy polymers. Additional studies are in progress to more extensively probe these failure modes in crosslinked and noncrosslinked resist systems, and predictive failure models for such materials are in development.

IV. CONCLUSIONS

The critical stress at the point of pattern collapse behavior of a model negative tone and positive tone resist has been studied in detail as a function of feature width and film thickness. It is observed that the pattern collapse performance of the model negative tone material is far superior to that of the model positive tone resist, with the negative tone resist being able to withstand stress levels that are roughly a factor of 2–3 times larger at equivalent resist film thicknesses and feature widths. Such a difference in critical stress translates into the ability to either utilize a film that is 1.4 to 1.7 times thicker in the case of the 4-Ep to pattern equivalent feature sizes as compared to the ESCAP-1 resist or to pattern features that are 30%–40% smaller in critical dimension for 4-Ep at equivalent resist feature heights as compared to ESCAP-1 before collapse becomes a problem. Such an enlargement of the lithographic process window with respect to pattern collapse thus serves as one motivation for further exploration of improved negative tone resists based on crosslinking for high resolution patterning. A strong decrease in critical stress with reducing feature width is also observed for the ESCAP-1 resist for feature widths below approximately 70–80 nm. This result suggests that the thin film effects observed in other work, in which the modulus of polymer films is observed to reduce with reducing film thickness below a critical thickness, can also have a dramatic effect on the effective mechanical response of small polymeric resist features. In contrast, the 4-Ep resist exhibits a minor dependence of critical stress on film thickness, suggesting that such thin film or confinement (i.e., high surface to volume) effects are not as significant in networked polymer systems. Thus, based on these results and similar studies with other materials, it is suggested that negative tone resist materials based on crosslinking imaging mechanisms that produce networked polymer features are very attractive in terms of providing resist solutions with significantly improved resistance to pattern collapse.

ACKNOWLEDGMENTS

The authors would like to gratefully acknowledge Intel Corporation for funding this work and Steve Putna, Todd Younkin, and Wang Yueh at Intel for helpful discussions on the subject. The authors would also like to thank Ralph Dammel and AZ Electronic materials for the donation of the aqueous developers, and JSR for the donation of the ESCAP-1 resin used in these studies.

[1]C. Martin, G. Rius, A. Llobera, A. Voigt, G. Gruetzner, and F. Pérez-Murano, Microelectron. Eng. **84**, 1096 (2007).
[2]J. Greener, W. Li, J. Ren, D. Voicu, V. Pakharenko, T. Tang, and E. Kumacheva, Lab Chip **10**, 522 (2010).
[3]G. Murillo, Z. J. Davis, S. Keller, G. Abadal, J. Agusti, A. Cagliani, N. Noeth, A. Boisen, and N. Barniol, Microelectron. Eng. **87**, 1173 (2010).
[4]C. S. Sharma, A. Sharma, and M. Madou, Langmuir **26**, 2218 (2010).
[5]B. Bilenberg, S. Jacobsen, M. S. Schmidt, L. H. D. Skjolding, P. Shi, P. Boggild, J. O. Tegenfeldt, and A. Kristensen, Microelectron. Eng. **83**, 1609 (2006).
[6]T.-H. Oh, R. Ganesan, J.-M. Yoon, and J.-B. Kim, Proc. SPIE **6153**, 61532G (2006).
[7]H. Sailer, A. Ruderisch, D. P. Kern, and V. Schurig, Microelectron. Eng. **73–74**, 228 (2004).
[8]H. Sailer, A. Ruderisch, W. Henschel, V. Schurig, and D. P. Kern, J. Vac. Sci. Technol. B **22**, 3485 (2004).
[9]R. A. Lawson, L. M. Tolbert, T. R. Younkin, and C. L. Henderson, Proc. SPIE **7273**, 72733E (2009).
[10]R. A. Lawson, C.-T. Lee, C. L. Henderson, R. Whetsell, L. Tolbert, and W. Yueh, J. Vac. Sci. Technol. B **25**, 2140 (2007).
[11]R. A. Lawson, C.-T. Lee, L. M. Tolbert, T. R. Younkin, and C. L. Henderson, Microelectron. Eng. **86**, 734 (2009).
[12]R. A. Lawson, D. E. Noga, T. R. Younkin, L. M. Tolbert, and C. L. Henderson, J. Vac. Sci. Technol. B **27**, 2998 (2009).
[13]R. A. Lawson, C.-T. Lee, W. Yueh, L. Tolbert, and C. L. Henderson, Microelectron. Eng. **85**, 959 (2008).
[14]Cheng-Tsung Lee, Mingxing Wang, Nathan D. Jarnagin, Kenneth E. Gonsalves, Jeanette M. Roberts, Wang Yueh, and C. L. Henderson, Proc. SPIE **6519**, 65191E (2007).
[15]C. M. Stafford, B. D. Vogt, C. Harrison, D. Julthongpiput, and R. Huang, Macromolecules **39**, 5095 (2006).